Neurochemistry International 131 (2019) 104538

Contents lists available at ScienceDirect

Neurochemistry International

journal homepage: www.elsevier.com/locate/neuint

Astrocyte culture models: Molecular and function characterization of primary culture, immortalized astrocytes and C6 glioma cells

Fabiana Galland[a], Marina Seady[a], Jessica Taday[a], Soraya Soubhi Smaili[b], Carlos Alberto Gonçalves[a], Marina Concli Leite[a,*]

[a] Departamento de Bioquímica, Instituto de Ciências Básicas da Saúde, Universidade Federal do Rio Grande do Sul, Porto Alegre, Brazil
[b] Departamento de Farmacologia da Escola Paulista de Medicina, Universidade Federal de São Paulo, São Paulo, Brazil

ARTICLE INFO

Keywords:
Astrocyte culture
C6 cells
Immortalized astrocytes
Astrocyte function

ABSTRACT

The understanding of the physiology of astrocytes and their role in brain function progresses continuously. Primary astrocyte culture is an alternative method to study these cells in an isolated system: in their physiologic and pathologic states. Cell lines are often used as an astrocyte model, since they are easier and faster to manipulate and cost less. However, there are a few studies evaluating the different features of these cells which may put into question the validity of using them as astrocyte models. The aim of this study was to compare primary cultures (PC) with two cell lines - immortalized astrocytes and C6 cells, in terms of protein characterization, morphology and metabolic functional activity. Our results showed, under the same culture condition, that immortalized astrocytes and C6 are positive for differentiated astrocytic markers (eg. GFAP, S100B, AQP4 and ALDH1L1), although expressing them in less quantities then primary astrocyte cultures. Glutamate metabolism and cell communication are reduced in proliferative cells. However, glucose uptake is elevated in C6 lineage cells in comparison with primary astrocytes, probably due to their tumorigenic origin and high proliferation rate. Immortalized astrocytes presented a lower growth rate than C6 cells, and a similar basal morphology as primary astrocytes. However, they did not prove to be as good reproductive models of some of the classic astrocytic functions, such as S100B secretion and GFAP content, especially while under stimulation. In contrast, C6 cells presented similar results in comparison to primary astrocytes in response to stimuli. Here we provide a functional comparison of three astrocytic models, in an attempt to select the most suitable model for the study of astrocytes, optimizing the research in this area of knowledge.

1. Introduction

Many important advances in the knowledge of astrocytes have been facilitated due to the isolation of these cells in culture (Lange et al., 2012). Primary astrocyte cultures enable the study of these cells in basal and neurotoxic conditions. Although this model may be limited by being an isolated system, it has been demonstrated recently that, under standard protocol, it shares similar gene expression characteristics when compared with freshly isolated astrocytes (Hertz et al., 2017). Astrocyte culture is a potent instrument to study mechanistic features in well-controlled conditions, such as calcium signaling, the release and uptake of gliotransmitters, as well as morphologic and biochemical changes. This model may also help in the development of new drugs for neurodegenerative diseases.

However, even though these advantages exist, the isolation of the primary astrocyte culture is a laborious process, both in terms of time consumption and high maintenance costs. Besides, it generates variable results since astrocytes are highly heterogeneous cells, making it difficult to compare results among different research groups. An alternative is the use of cell lines, such as C6 glioma cells (ATCC CCL-10), which is a highly used model. These cells are isolated from a rat brain tumor (Benda et al., 1968) and are used as astrocyte-like cell line in high passages (over a hundred) due to the increased expression of some astrocyte markers, as glial fibrillary acidic protein (GFAP), S100B, glutamine synthetase (GS) and glutamate transporters (Baber and Haghighat, 2010; Haghighat, 2005; Parker et al., 1980; Raju et al., 1980; Tabuchi et al., 1982). Another model to study astrocytes in culture is immortalized astrocytes, which are genetically transformed cells with higher proliferative rate (Frisa and Jacobberger, 2002; Furihata et al., 2016; Morikawa et al., 2001). These cells have the advantage of originating from a primary astrocyte culture and not from a tumor. Both transformed cells could provide more homogeneous features than

* Corresponding author. Depto Bioquímica, ICBS, UFRGS, Ramiro Barcelos, 2600-anexo, Porto Alegre, RS, 90035-003, Brazil.
E-mail address: marina.leite@ufrgs.br (M.C. Leite).

https://doi.org/10.1016/j.neuint.2019.104538
Received 20 May 2019; Received in revised form 10 August 2019; Accepted 17 August 2019
Available online 17 August 2019
0197-0186/

primary astrocyte cell cultures, originating from clones. Furthermore, they are faster and easier to manipulate than primary cultures once they can be stocked and thawed.

Despite these facilities, the use of cell lines has been questioned in the literature due to their glioma features and certain different characteristics from primary culture which put into question the validity of these cell line models (Haghighat and McCandless, 1997a, 1997b; Leite et al., 2009; Nardin et al., 2007; Tabernero et al., 2006). There are no data in the literature that show a complete and integrative evaluation of primary astrocytes culture (PC) as compared to immortalized astrocytes (IA) and C6 glioma cell line (C6). Here we show a comparative analysis of these three models with regards to their morphological and functional features under the same growth conditions. We show differences in the cell morphology and protein expression characteristics of astrocytes, such as GFAP, S100B, aldehyde dehydrogenase 1 family, member L1 (ALDH1L1), aquaporin-4 (AQP4) and potassium channel-4 (Kir4.1). Furthermore, glutamate metabolism was evaluated by glutamate uptake, protein expression of its transporters (EAAT1 and EAAT2), glutamine synthetase activity and GSH content. Glucose metabolism was also assessed using H^3-glucose uptake and its transporter protein content (GLUT1). We also evaluated the communication of these cells by gap junction, checking Cx43 expression and its coupling. In addition, we showed the responsiveness of these cell models under toxic stimuli, evaluating astrocytic activation through GFAP content and S100B secretion, glutamate and glucose metabolism and inflammatory cytokine. This study contributes to the evaluation of different model of astrocyte culture, optimizing the research in this area of knowledge and a better understanding of astrocyte cell physiology.

2. Materials and methods

2.1. Materials

Poly-L-lysine, methylthiazolyldiphenyl-tetrazolium bromide (MTT), neutral red, glutathione standard, phthaldialdehyde, lipopolysaccharides from *Escherichia coli* (LPS) 055:B5, L-glutamate, *o*-phenylenediamine (OPD), γ-glutamylhydroxamate acid, N-methyl-d-glucamine and aminoguanidine hemisulfate salt (AG) were purchased from Sigma [St. Louis, USA]. Lipofectamine, Fetal calf serum (FCS), Dulbecco's modified Eagle's medium (DMEM) and other materials for cell culture were purchased from Gibco [Carlsbad, USA]. l-[2,3-^{3}H] glutamate was purchased from Amersham International [Buckinghamshire, United Kingdom] and deoxy-d-glucose, 2-[^{3}H(G)] (10 Ci/mmol) was purchased from American Radiolabeled Chemicals, Inc. [Saint Louis, USA]. Lucifer Yellow was purchased from Invitrogen, Life Technology Corporation [Carlsbad, USA]. Antibodies obtained from Sigma [St. Louis, USA] were: anti-S100B (SH-B1) and anti-GFAP. Human GFAP from Calbiochem. Antibodies obtained from Santa Cruz Biotechnology [Santa Cruz, USA]: polyclonal anti-RAGE (N16), anti-glutamine synthetase, polyclonal anti-Kir4.1, anti-BDNF, anti-GLUT1 and anti-goat IgG-R. Antibodies obtained from Chemicon [Temecula, USA]: polyclonalanti-AQP-4 antibody and anti-conexin-43. Monoclonal anti-aldehyde dehydrogenase family 1-member L1 was obtained from Neuromab (Davis, USA). Polyclonal anti-S100B and anti-rabbit peroxidase were purchased from DAKO [São Paulo, Brazil] and GE [Little Chalfont, United Kingdom], respectively. Antibodies anti-EAAT1 and EAAT2 were purchased form Abcam [Cambridge, USA], and anti-actin from Merck Millipore Corporation [São Paulo, Brasil].

2.2. Astrocytes primary cell culture

Primary astrocyte cultures from Wistar rats were prepared as previously described by Gottfried et al. (2002). Procedures were carried out in accordance with the NIH Guide for the Care and Use of Laboratory Animals and were approved by the local authorities. Briefly, cerebral cortices of newborn Wistar rats (1–2 days old) were removed and mechanically dissociated in Ca^{2+}- and Mg^{2+}-free balanced salt solution, pH 7.4, containing (in mM): 137 NaCl; 5.36 KCl; 0.27 Na_2HPO_4; 1.1 KH_2PO_4 and 6.1 glucose. The cortices were cleaned of meninges and mechanically dissociated by sequential passage through a Pasteur pipette. After centrifugation at 300 × *g* for 5 min, the pellet was suspended in DMEM (pH 7.6) supplemented with 8.39 mM HEPES, 23.8 mM $NaHCO_3$, 0.1% amphotericin B, 0.032% gentamicin and 10% fetal calf serum (FCS). Cells were plated onto 12 or 24-well- plates (800.000 and 300.000 cells/well, respectively) pre-treated with poly-L-lysine. Cultures were maintained in DMEM containing 10% FCS in 5% CO_2/95% air at 37 °C. The medium was changed every 3–4 days. Cells were allowed to grow to confluence and used at 21 days *in vitro*. Immunocytochemistry was made with pre-confluent cells, approximately 10 days *in vitro*, seeded on coverslips covered with poly-L-lysine. The purity of astrocyte primary cell culture was more than 95%, assessed by immunocytochemistry (GFAP/S100B double staining). We were unable to label neurons or microglia, using anti-NeuN or anti-Iba-1 respectively.

2.3. C6 glioma cell culture

The C6 glioma cell line was obtained from the American Type Culture Collection (Rockville, MD). Late passage cells (i.e. after at least 100 passages) were seeded in 25 cm^2 flasks and cultured in DMEM 10% FCS (same medium as described for astrocytes primary culture). Exponentially growing cells were detached from the culture flasks using 0.05% trypsin/ethylenediaminetetraaceticacid (EDTA) and seeded on coverslips (immunocytochemistry) on 12 or 24-well plates. Cells were allowed to grow to confluence and used in 3 days *in vitro*.

2.4. Culture of immortalized astrocytes

Immortalized astrocytes were donated by Professor Soraya Soubhi Smaili (Laboratory of Calcium Signaling and Cell Death). Briefly, astrocyte primary culture with 11 days *in vitro* was transfected with a mixture of 3 μg of pSV3-neo plasmid and 10 μg of lipofectamine over a period of 5 h. The plasmid pSV3 contains the gene for the large SV40 T antigen, which interferes with the expression of tumor suppressor proteins. As a control, cells were also transfected with GFP plasmid (pcDNA3 vector). Four days after transfection, the antibody G418 was added for the selection of neomycin-resistant colonies. The medium was changed every 3–4 days and the concentration of G418 was gradually increased from 200 to 800 μg/mL. After 3 weeks, isolated colonies were selected and seeded on 24-well plates and gradually expanded in 75 cm^2 flasks. The transfected cells were maintained in DMEM with 10% FCS, 1% penicillin/streptomycin and 200 μg/mL of G418. Immortalized astrocytes from 10 to 30 passages were used in these experiments.

2.5. Immunocytochemistry

Immunocytochemistry was performed as described previously by (Lasič et al., 2016) with some modifications. Briefly, cell cultures were fixed with 4% paraformaldehyde/4% sucrose for 10 min and permeabilized with 0.1% Triton X-100 in PBS for 20 min at room temperature. After blocking 1 h with 2% albumin bovine, the cells were incubated overnight with anti-GFAP, anti-S100B or anti-actin. For PC, antibodies were incubated at a concentration of 1:1000 and for IA and C6, antibodies were incubated at 1:250. After a 3-stage washing with PBS, specific secondary antibodies conjugated with Alexa Fluor 488 (green staining) or 568 (red staining) were incubated for 1 h at room temperature. For all the immunostaining-negative controls, the reactions were performed by omitting the primary antibody. No reactivity was observed when the primary antibody was excluded. Cell nuclei were stained with 0.2 mg/mL of 49,69-diamidino-2 phenylindole (DAPI). The cells were visualized with a Nikon inverted microscope and the

images were transferred to a computer with a digital camera (Sound Vision Inc.).

2.6. S100B measurement

S100B was measured by ELISA, as previously described by Leite et al. (2008). Briefly, 50 µl of sample (previously homogenized and diluted) plus 50 µl of tris buffer 50 mM were incubated for 2 h on a microtiter plate previously coated overnight with monoclonal anti-S100B and blocked for 1 h with 2% albumin from chicken egg. Polyclonal anti-S100 was incubated for 30 min and then peroxidase-conjugated anti-rabbit antibody was added for a further 30 min. The microtiter plate was rinsed three times between each step with a wash solution. O-phenylenediamine was added for 30 min and the colorimetric reaction was determined at 492 nm. The standard S100B curve ranged from 0.002 to 1 ng/mL.

2.7. GFAP measurement

The ELISA for GFAP was carried out, as previously described by Tramontina et al. (2007). Homogenates of cell culture (100 µl) previously diluted in TBS or standard human GFAP ranging from 0.1 to 5 ng were incubated in microtiter plates for 24 h at 4 °C. After blocking with 5% milk-TBS (M-TBS) for 2 h at room temperature, a rabbit polyclonal anti-GFAP (dilution in 0.5% M-TBS) was incubated for 1 h. Then, secondary antibody conjugated with peroxidase was incubated for 1 h at room temperature. The microtiter plate was rinsed three times between each step with a wash solution. O-phenylenediamine was added for 30min and the colorimetric reaction was determined at 492 nm.

2.8. Glutamine synthetase activity

The enzymatic activity of glutamine synthetase was determined using the procedures described previously by Minet et al. (1997), with modifications. Briefly, homogenized samples diluted in 50 mM imidazole were incubated with (mM): 50 imidazole, 50 hydroxylamine, 100 L-glutamine, 25 sodium arsenate dibasic heptahydrate, 0.2 ADP, 2 manganese chloride, pH 6.2 for 15 min at 37 °C. The reaction was stopped by the addition of 0.2 mL of 0.37 M $FeCl_3$, 200 mM trichloroacetic acid, and 0.67 M HCl. After centrifugation, the absorbance of the supernatant was measured at 540 nm and compared to the absorbance generated by standard quantities of γ-glutamyl hydroxamate acid diluted in the same solution as the samples. Glutamine synthetase activity was expressed as µmol/h/mg protein.

2.9. GSH

Reduced glutathione content was determined as previously described (Browne and Armstrong, 1998). Briefly, the samples were homogenized in sodium phosphate buffer (0.1 M, pH 8.0) containing 5 mM EDTA and protein was precipitated with 1.7% meta-phosphoric acid. Supernatant was assayed with o-phthaldialdehyde (1 mg/mL methanol) at room temperature for 15 min. Fluorescence was measured using excitation and emission wavelengths of 350 and 420 nm, respectively. A calibration curve was employed using standard GSH solutions (0–500 µM).

2.10. Glutamate uptake assay

Glutamate uptake was measured, as previously described by Gottfried et al. (2002) with some modifications (Thomazi et al., 2004). Cell cultures were incubated at 37 °C in Hank's balanced salt solution (HBSS) containing (in mM): 137 NaCl, 5.36 KCl, 1.26 $CaCl_2$, 0.41 $MgSO_4$, 0.49 $MgCl_2$, 0.63 $Na_2HPO_4{\cdot}7\ H_2O$, 0.44 KH_2PO_4, 4.17 $NaHCO_3$ and 5.6 glucose, pH 7.4. The assay was started by the addition of 0.1 mM L-glutamate and 0.66 µCi/mL L-[2,3-^{3}H] glutamate. Incubation was stopped after 7 min for PC and 10 min for IA and C6 cells, by removing the medium and rinsing the cells three times with ice cold HBSS. The cells were then lysed in a 0.5 M NaOH solution. Sodium-independent uptake was determined using *N*-methyl-D-glucamine instead of NaCl. Sodium dependent glutamate uptake was obtained by subtracting the non-specific uptake from the total uptake to obtain the specific uptake. Radioactivity was measured in a scintillation counter. Results were expressed as nmol/mg protein/min.

2.11. Glucose uptake assay

Glucose uptake was measured as previously described (Pellerin and Magistretti, 1994), with modifications. Cell cultures were rinsed in HBSS. Subsequently, cells were incubated at 35 °C in HBSS (described above). The assay was initiated by the addition of 0.1 µCi/well deoxy-d-glucose, 2-[^{3}H(G)]. The incubation was stopped after 15 min by removing the medium and rinsing the slices three times with ice-cold HBSS. The cells were then lysed in a solution containing 0.5 M NaOH. Glucose uptake was calculated by subtracting the non-specific uptake, obtained by using the glucose transporter inhibitor, cytochalasin B (10 µM), from the total uptake in order to obtain the specific uptake. Radioactivity was measured using a scintillation counter. Results were expressed as nmol/mg protein/min.

2.12. TNF alpha measurement

TNF-α was measured using a commercial ELISA colorimetric kit (eBioscience, Inc. San Diego, USA) in the supernatant of cell cultures, following the manufacturer's instructions.

2.13. Western blot analyses

Cell cultures were homogenized in a sample buffer (0.0625 M tris–HCl, pH 6.8, 2% (w/v) SDS, 5% (w/v) b-mercaptoethanol, 10% (v/v) glycerol, 0.002% (w/v) bromophenol blue) and subsequently boiled and centrifuged. Equal amounts (25 µg) of total protein was electrophoresed in a 12% (w/v) SDS–polyacrylamide gel. The separated proteins were blotted onto a nitrocellulose membrane. Membranes were incubated in TBS-T (20 mmoL/L Tris–HCl, pH 7.5, 137 mmoL/L NaCl, 0.05% (v/v) Tween-20) containing 2% (w/v) bovine albumin for 1 h at 4 °C. Subsequently, the membranes were incubated overnight, at 4 °C, with the appropriate primary antibody in a dilution (1:5000): anti-GFAP, anti-vimentin, anti-GS, anti Kir4.1, anti-AQ-4, anti ALDH1L1, anti-Cx43, anti-BDNF, anti-EAAT1, anti-EAAT2 or anti-GLUT-1. Membranes were then rinsed with TBS-T and exposed to horseradish peroxidase-linked anti-IgG antibodies for 1 h at 4 °C.Equivalent loading of each sample was confirmed with anti-actin. The chemiluminescence signal was detected using an ECL kit from Amersham and evaluated in the luminescence image analyzer (Image Quant LAS4000 from GE). The luminescence signal differences were analyzed using ImageJ software.

2.14. Cell coupling

Scrape loading/dye transfer was carried out as previously described (Leite et al., 2009). After treatment, the conditioned incubation medium was removed and saved. The cultures were quickly and carefully rinsed in Ca^{+2}-free HBSS to prevent uncoupling of the cells as a result of high Ca^{2+} levels. Two parallel scrapes were performed with a scalpel blade in the Ca^{+2} free HBSS with 0.1% (w/v) Lucifer yellow at room temperature. Disruption of the cell membrane allows the dye to permeate the cells and to diffuse to surrounding cells through GJ channels. The dye was rinsed away with HBSS after 1 min. The conditioned incubation medium was reintroduced, and cultures were left for 7 min. After that, cells were viewed with a Nikon inverted microscope and images transferred to a computer with a digital camera. All images

are representative fields from at least three experiments carried out in triplicate.

2.15. MTT reduction assay

Cells were incubated with 50 µg/mL methylthiazolyldiphenyl-tetrazolium bromide (MTT) during the last 30 min of incubation at 37 °C. Afterwards, the medium was removed and MTT crystals were dissolved in DMSO. Absorbance values were measured at 560 and 650 nm. The reduction of MTT was calculated as (abs at 560 nm) − (abs at 650 nm) and expressed as a percentage of basal.

2.16. Protein determination

Protein content was measured by Lowry's method, modified by Peterson, using bovine serum albumin as standard (Peterson, 1977).

2.17. Statistical analysis

Parametric data are reported as means ± standard errors and were analyzed by *t*-test or one-way analysis of variance (ANOVA) followed by Tukey's post-hoc, using SPSS-16.0. Tests are specified in the legends, with the level of significance set at $p < 0.05$.

3. Results

Cell astrocyte morphology was evaluated with the label of actin, GFAP and S100B proteins (Fig. 1). PC and IA showed similar polygonal shape with few cell processes. Actin label revealed organized filaments in both cell types. In contrast, C6 glioma cells presented an elongated body with diffuse actin fibers. In contrast to IA, PC and C6 presented morphological alterations induced by forskolin 10 µM stimulus. PC showed stellated characteristic shape and C6 showed a cell body retraction with thin processes. As is known, an increase on GFAP/vimentin ratio during development is associated with astrocytic differentiation (Menet et al., 2001). In our study, IA and C6 showed the same GFAP/vimentin ration as PC, indicating a similar differentiation state (Fig. 2A).

Regarding the astrocytic markers, C6 and IA were positive, but showed reduced levels of GFAP, S100B, ALDHL1 and AQP4, compared to PC (Fig. 2 A, B, D and E). Interestingly, Kir4.1 showed similar levels in all tested cell models (Fig. 2F).

Glutamate metabolism was assessed by measuring glutamine synthetase (GS) and glutamate transporters content (EAAT1 and EAAT2), as well as GS activity and glutamate uptake. All these measurements were reduced in IA and C6 cells (Fig. 3A–E). Interestingly, GSH content, which is the main antioxidant in astrocytes and whose biosynthesis also depends on glutamate content, was produced in equivalent amounts by PC, IA and C6 (Fig. 3F).

Glucose metabolism was evaluated through the measurement of glucose transporter and uptake. In these analysis, C6 glioma cells showed higher rate of glucose uptake than PC and IA (Fig. 4A). Despite this data, IA and C6 presented lower levels of glucose transporter (GLUT-1) content as compared to PC (Fig. 4B).

Astrocytic communication is essential for many of their functions (Rouach et al., 2002). This communication was evaluated by the analysis of conexin-43 content, the most abundantly expressed connexin in astrocyte cultures, and by a scrap loading assay carried out with Lucifer Yellow dye. Both analyses revealed impaired gap junction communication in IA and C6 cells when compared to PC (Fig. 5 A and B).

Considering that the three models of astrocytes presented variation in basal protein profile, we wondered if they would respond differently under the same stimulus. We used well described stimuli to interfere with astrocyte function. As shown in Table 1, the three cell models responded in a similar way under stimuli relative to glucose and glutamate uptake, as well as TNFα secretion. However, IA was unaffected by stimuli regarding S100B secretion, GS activity and GSH content, in opposite to PC and C6 which had similar response. Interestingly, the increase in GFAP under LPS stimuli observed in PC was not shown in either IA nor C6. Viability of the cells under all stimuli was not compromised, based on MTT reduction assay (data not shown).

4. Discussion

4.1. Morphology and plasticity evaluation

Astrocyte morphology and plasticity may be critical in the regulation of extracellular microenvironment and synaptic activity (De Pittà et al., 2016; Ostroff et al., 2014). In this study, morphological evaluation in basal conditions showed a similar polygonal shape between PC and IA. In contrast, C6 cells showed a fusiform or triangular cell body and irregular actin network, which was previously associated with glioma invasiveness (Zhou et al., 2008). Although C6 have been used in high passages in our work, these cells have a tumoral origin and may

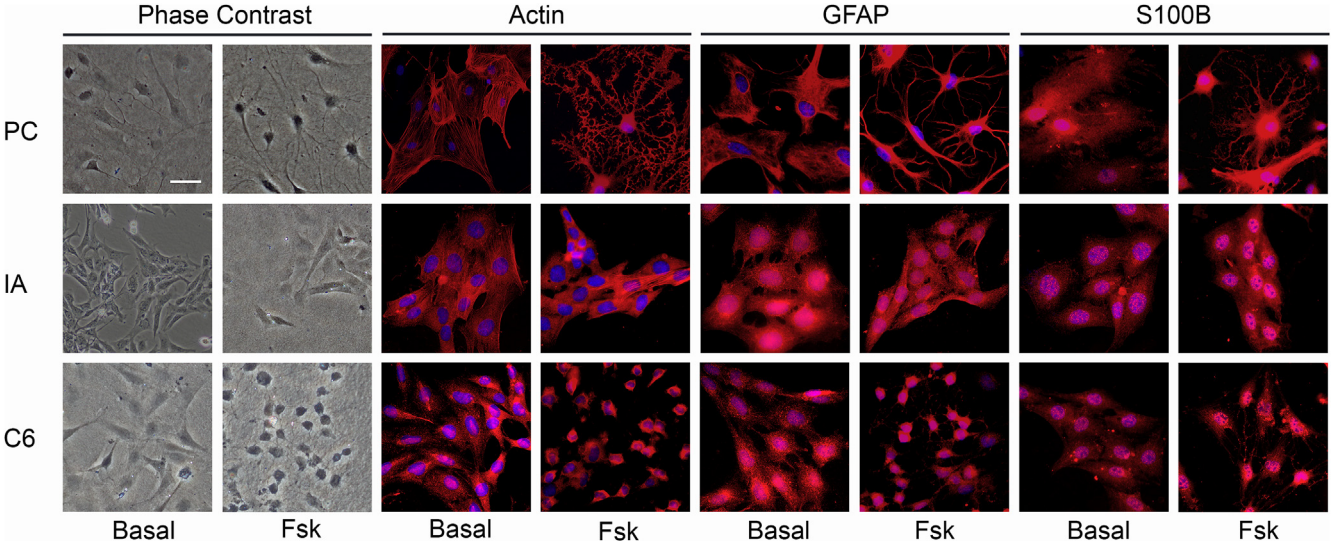

Fig. 1. Morphological evaluation of PC, C6 and IA. Immunocytochemistry for actin, GFAP and S100B was done in basal and forskolin 10 µM stimulated conditions (15 min) in primary culture (PC), immortalized astrocytes (IA) and C6 cells (C6). Scale bar = 50 µm.

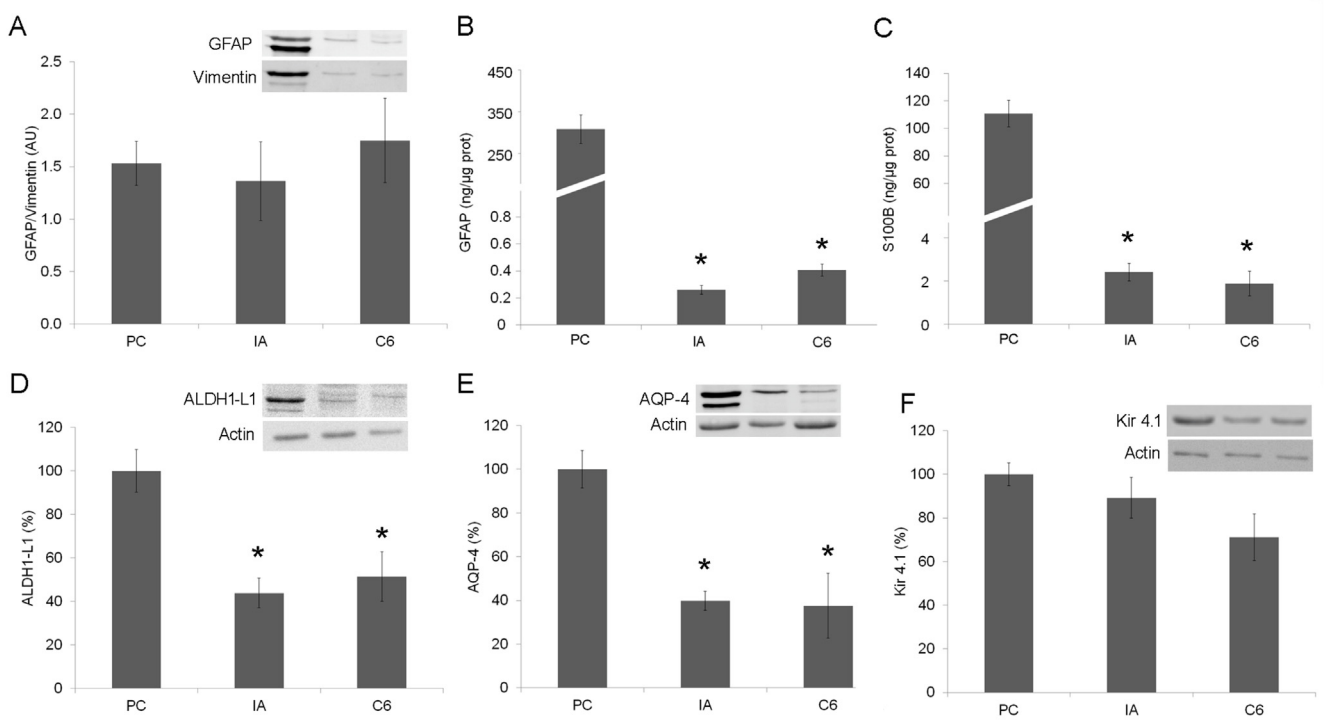

Fig. 2. Protein profile of astrocytic markers in PC, IA and C6. The content of characteristic proteins of astrocytes was analyzed under basal conditions in PC, IA and C6. GFAP-vimentin ratio was measured by Western blot (A); GFAP (B) and S100B (C) content was measured by ELISA; ALDH1L1 (D); AQP4 (E) and Kir4.1 (F) content was measured by Western blot. Representative immunoblots are shown in inserts. Each value is the mean (± standard error) from at least 5 experiments. Statistical analysis was performed by one-way ANOVA followed by Tukey's test, with a significance level of $p < 0.05$.

preserve some characteristics of transformed cells.

Under forskolin stimulus, which classically induces an increase in the intracellular content of cAMP, PC showed cell body retraction and prominent long processes as expected (Pinto et al., 2000). Under the same condition, C6 showed a cell body retraction, but sparse and thinner processes than PC. Even though IA are morphologically similar to PC, they were not affected by forskolin stimuli. Interestingly, primary astrocyte culture was shown to lose processes after subculturing (Passaquin et al., 1994) which may explain part of IA unresponsiveness. Similar to our results, dibutyryl-cAMP did not induce up-regulation of GFAP in immortalized cell lines as did to C6 and PC (Geller and Dubois-Dalcq, 1988). Furthermore, astrocyte hypertrophy is highly dependent on GFAP content which is already shown to be reduced in lineage cells (Wilhelmsson et al., 2004) and was confirmed by this study. In summary, our results show that morphology plasticity may be compromised in IA, making this cell line a disadvantageous model for this evaluation.

4.2. Protein expression profile of astrocyte models

Astrocytes are functional and molecularly heterogeneous cells. However, they have some protein markers, like S100B and GFAP (Brozzi et al., 2009; Eng, 1985; Van Eldik and Wainwright, 2003). C6 and IA were positive for both markers, although in significantly less quantities than PC. Similar results were previously observed in other works (Furihata et al., 2016; Groves et al., 1993; Morikawa et al., 2001; Raju et al., 1980; Tabuchi et al., 1982). Besides these markers, we also evaluated ALDH1L1 protein which has been used as a new astroglial marker (Souza et al., 2013; Yang et al., 2011). Although this protein participates in folate metabolism, interfering in cell division and growth (Krupenko, 2009), IA and C6 cells showed reduced levels of ALDH1L1 compared to PC. The same result was seen with AQP4 levels, which is widely expressed in astrocyte membranes (Papadopoulos and Verkman, 2013).

The reduced levels of important astrocytic markers in IA and C6 cells may be explained by their high proliferative profile. In this sense, both cell lines may invest more in the synthesis of proteins related to cell proliferation instead of specific astrocytic markers. It is known the level of any specific protein inside cells is dynamic. Gene expression may vary dependent on cell density or cell cycle transition time. For example, a decrease in proliferative associated genes is expected in confluent cells or, an upregulation in genes associated with cell differentiation (Frisa and Jacobberger, 2002). The attenuation in proliferative abilities may allow the cell to undergo a more differentiated status. Therefore, it is important in this analysis, and in any other study that uses these cell models, to maintain a confluence pattern in order to reach gene expression stability.

Interestingly, Kir4.1 channel, which is also a glial specific protein (Seifert et al., 2016), showed similar content in all tested cell types. However, potassium conductance has been shown to be impaired in gliomas due to a nucleus membrane localization instead of cellular membrane (Olsen and Sontheimer, 2008). Therefore, similar protein expression does not necessarily represent Kir4.1 function.

4.3. Functional characterization of glutamate metabolism

An impaired glutamate metabolism in astrocytes may compromise the glutamate-glutamine cycle and many brain functions as seen in neurodegenerative diseases (Benarroch, 2010). Recently it was shown that astrocyte glutamate uptake depends on GS activity, which ensures an efficient clearance of glutamate captured by EAATs (Trabelsi et al., 2017). Therefore, rather than observe only expression, as seen in earlier studies (Baber and Haghighat, 2010; Furihata et al., 2016), our analysis evaluated the functionality of this clearance mechanism. We found a reduced glutamate metabolism in IA and C6 cells compared to PC. Although the basal expression of glutamate transporters in cell lines is not so different to PC, its functionality was extremely low, suggesting that EAAT1 and EAAT2 could be poorly located in plasmatic membrane in these cells. It is important to note that other studies have not detected

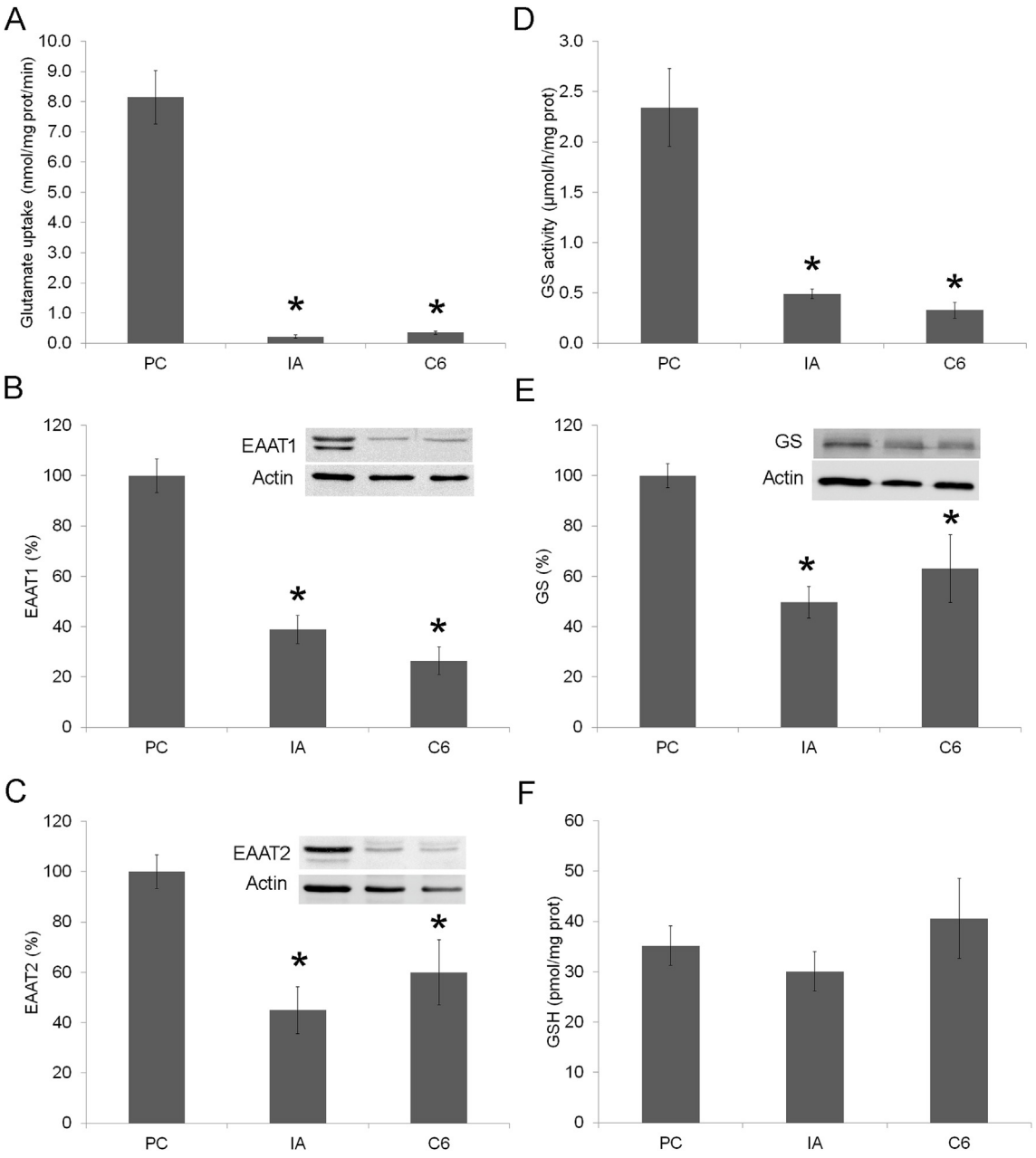

Fig. 3. Glutamate metabolism in PC, IA and C6 cells. Glutamate uptake was assessed under basal conditions by a radiometric assay (A). The immunocontent of EAAT1 (B) and EAAT2 (C) was measured by Western blot. Glutamine synthetase activity was measured by a colorimetric assay (D) and GS immunocontent by Western blot analysis(E). GSH content was measured by fluorimetric assay (F). Representative immunoblot are shown in inserts. Each value is the mean (± standard error) from at least 5 experiments. Statistical analysis was performed one-way ANOVA followed by Tukey's test, with a significance level of $p < 0.05$.

glutamate transporters in lineage cells, however this was analyzed in C6 low passages, in opposed to our cells, that were subcultured at least 100 times (Palos et al., 1996; Vanhoutte and Hermans, 2008). The mechanistic reason for the switching of C6 from a glioma to a differentiated astrocyte model is still unknown. Interestingly, EAAT2 overexpression was shown to reduce the proliferative rate of C6 cells under glutamate stimulus, showing a negative correlation between glutamate transporters and cell proliferation (Vanhoutte and Hermans, 2008).

GSH production gives astrocytes a high capacity to oxidative defense in the brain (Matés et al., 2002) and all tested cell types showed similar GSH content. It is known that GSH production is dependent on glutamate content. Considering that glutamate uptake and GS activity were lower in IA and C6 cells than PC, we can assume that glutamate is mainly directed to GSH production in these cell lines (McKenna et al., 1996). Therefore, these pathways may be differently controlled in PC, IA and C6 cells. Corroborating this idea, the Xc-cysteine/glutamate antiporter system has been shown to be overexpressed in glioma cells compared with normal astrocytes, contributing to their growth, survival and expansion (Bridges et al., 2012). Moreover, high GSH production may protect glioma cells against the high oxidative metabolism observed in proliferative cells (Marie and Shinjo, 2011; Pallardó et al., 2009).

4.4. Energy metabolism and gap junction communication in astrocytes

Astrocytes represent a key element in brain energy homeostasis. Most glucose captured by astrocytes is driven to glycogen stores and/or is converted to lactate for neuronal export (Bouzier-Sore and Pellerin, 2013; Pellerin, 2008). Although the main glucose transporter in astrocyte (GLUT-1) is under expressed in IA and C6 compared to PC, glucose

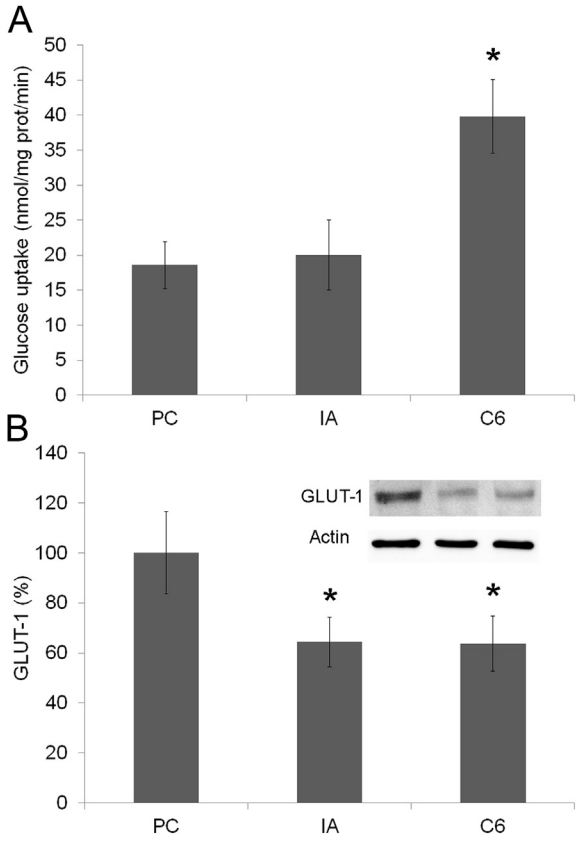

Fig. 4. Glucose metabolism in PC, IA and C6 cells. Glucose uptake was assessed under basal conditions by a radiometric assay (A). The immunocontent of GLUT-1 was measured by Western blot (B). Representative immunoblot is shown in the insert. Each value is the mean (± standard error) from at least 5 experiments. Statistical analysis was performed one-way ANOVA followed by Tukey's test, with a significance level of $p < 0.05$.

uptake is more pronounced in C6 cells (Fig. 4). It is known that tumor derivative cells present the Warburg Effect, that is when glycolysis is the primary method of energy derivation. Therefore, they use much more glucose than normal cells (Labak et al., 2016). Accordingly, a previous study showed that C6 glioma cells utilize more glucose and produce less lactate than normal astrocytes (Haghighat and McCandless, 1997a). It was suggested that glucose may be used in another pathway such as the pentose phosphate shunt, which increases NADPH and GSH content produced by glutathione reductase activity (Dringen et al., 2015). In accordance with this, an increase in energy metabolism is common in proliferative cells (Marie and Shinjo, 2011).

Metabolic substrates, such as glucose, can cross astrocytic gap junctions and this communication is inversely associated with proliferative rate (Tabernero et al., 2006). Tumor cell lines are usually devoid of gap junction, and its presence is inhibited by tumor-promoting molecules (Budunova and Williams, 1994). In fact, C6 are known to have low levels of cell communication, which is in accordance with the low expression of Cx43 seen in our results and in previous studies (Liu et al., 2012; Rouach et al., 2002). Interestingly, an increase in gap junction communication decreases glucose uptake and proliferative rate in C6 cells (Tabernero et al., 2006). At the same time an inhibition of gap junction by endothelin stimulates the translocation and up-regulation of GLUT-1 from the intracellular pool to the plasma membrane in astrocytes (Sánchez-Alvarez et al., 2004). Thus, beyond the Warburg Effect, gap junction also may play an important role in glucose uptake regulation in proliferative cells.

4.5. Response of culture models to different stimuli

Some contradictory results are found in the literature when different models of astrocyte culture are submitted to the same treatment (Haghighat and McCandless, 1997a; Leite et al., 2009; Morikawa et al., 2001; Nardin et al., 2007). These varying results make the analysis difficult and raise doubt as to the validity of the model. Therefore, we tested how the three different models of astrocyte culture would respond to the same treatment. For that, we used stimuli that were already known in the literature to cause functional changes in primary culture. It is important to mention that variation in culture response may also be influenced by differences in culture procedure, such as medium composition, culture plate coating and days *in vitro* (Lange et al., 2012). These differences may interfere in gene expression and morphological variations (Passaquin et al., 1994). In fact, recently it was shown that extracellular matrix composition determines astrocyte responses to mechanical and inflammatory stimuli (Johnson et al., 2015). In this work, we applied the same procedures to all three cultured models, ensuring that the treatment effects observed were due to biological cell variation.

Overall, our results showed that PC and C6 cells respond similarly to the same stimulus, specifically in relation to S100B secretion, GSH content, glutamine synthetase activity, glucose and glutamate uptake and TNFα secretion (Table 1). Therefore, although they often presented differences in the basal amount of protein, the activation of these pathways appears to be similar, at least for the tested stimuli. In contrast, IA showed less reactivity, indicating that this transfected clone is not a good model for the study of certain astrocyte features. Recently, it was shown that p53 isoform, expressed in different passages, regulates astrocyte-mediated neuroprotection and neurodegeneration (Turnquist et al., 2016). Therefore, IA, that has p53 inhibition (due to the transfection process) may have compromised functionality. It is important to note that IA preserved the response to glutamate and glucose uptake, as well as TNF α secretion.

5. Conclusions

Based on our data, although PC is a more time-consuming and costly

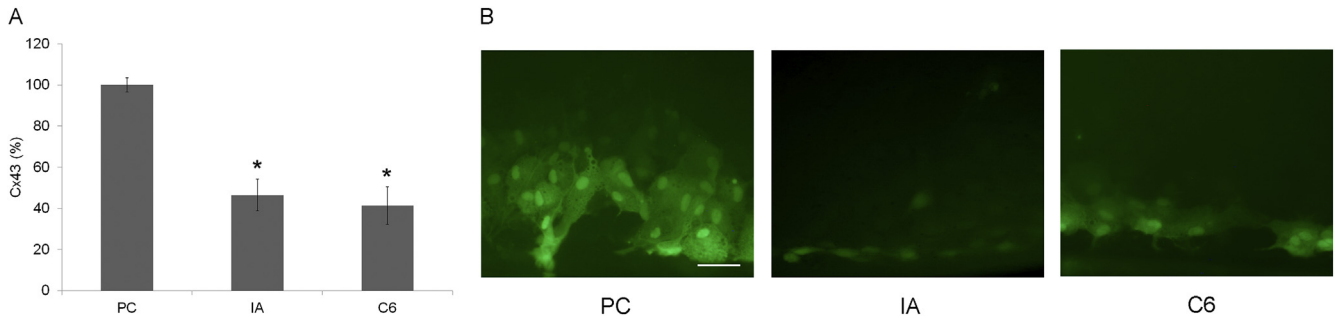

Fig. 5. Gap junction communication in PC, IA and C6. Conexin-43 immunocontent was evaluated under basal conditions by Western blot (A). Representative images of scrape loading with Lucifer yellow dye (B). Scale bar = 50 μm.

Table 1
Astrocytes culture response under stimulus.

Assay	Stimulus/time of incubation	PC	IA	C6
S100B secretion	LPS 1 μg/mL- 24 h [61]	↓ 77.6* ± 6.2%	– 121.5 ± 30%	↓ 37.5* ± 4.8%
GS activity	H_2O_2 50 μM - 3 h [62]	↓ 84.6* ± 3.4%	– 125 ± 11%	↓ 75.6* ± 8.9%
GSH content	H_2O_2 50 μM - 3 h [63]	↓ 70.2* ± 8.0%	– 91.4* ± 6.3%	↓ 66.9* ± 9.2%
Glucose uptake	S100B 0.1 ng/mL - 30 min [64]	↓ 67.6* ± 4.8%	↓ 78.6* ± 7.8%	↓ 66.8* ± 11.7%
Glutamate uptake	NH_3 5 mM - 24 h [65]	↓ 77.4* ± 7.0%	↓ 59.9* ± 9.1%	↓ 76.4* ± 8.5%
GFAP	LPS 1 μg/mL - 24 h [61]	↑ 178.1* ± 20%	– 81 ± 10.2%	– 122 ± 27%
TNFα secretion	LPS 10 μg/mL 24 h [61]	↑ 433.2 ± 55.5%	↑ 201.6 ± 75.0	↑ 225.6 ± 25.7

Astrocytes were treated with the indicated stimuli, and times and assays were performed. Stimuli were chosen in accordance with previews works which showed alteration in PC parameters. Numbers indicate the percentage in relation to controls. Arrows up (↑) indicate an increase, arrows down (↓) indicate a reduction in comparison to controls and traces (–) indicates no effect. Statistical analysis was performed by T-test, with a significance level of $p < 0.05$. Primary culture (PC), immortalized astrocytes (AI) and C6 glioma cell line (C6).

technique, its use as a reproductive model for astrocyte studies is undoubtedly preferential. However, the C6 cell line, although presenting certain limitations, seems to reproduce an astrocyte in a significant way. In summary, this work identified the limitations and advantages of each type of culture, providing a complete and integrative comparison of astrocytes function and optimizing the research in this area of knowledge. Besides, it highlighted the importance of validating cell culture models for each stimulus of interest, in order to choose an appropriate cell model, when the use of PC is not possible.

Acknowledgements

This work was supported by the Conselho Nacional de Desenvolvimento Científico e Tecnológico (CNPq), Coordenação de Aperfeiçoamento de Pessoal de Nível Superior (CAPES), Fundação de Amparo à Pesquisa do Estado do Rio Grande do Sul (FAPERGS) and Instituto Nacional de Ciência e tecnologia (INCT).

Appendix A. Supplementary data

Supplementary data to this article can be found online at https://doi.org/10.1016/j.neuint.2019.104538.

References

Baber, Z., Haghighat, N., 2010. Glutamine synthetase gene expression and glutamate transporters in C6-glioma cells. Metab. Brain Dis. 25, 413–418. https://doi.org/10.1007/s11011-010-9223-9.

Benarroch, E.E., 2010. Glutamate transporters: diversity, function, and involvement in neurologic disease. Neurology 74, 259–264. https://doi.org/10.1212/WNL.0b013e3181cc89e3.

Benda, P., Lightbody, J., Sato, G., Levine, L., Sweet, W., 1968. Differentiated rat glial cell strain in tissue culture. Science (80-.) 161, 370–371. https://doi.org/10.1126/science.161.3839.370.

Bouzier-Sore, A.K., Pellerin, L., 2013. Unraveling the complex metabolic nature of astrocytes. Front. Cell. Neurosci. 7, 179. https://doi.org/10.3389/fncel.2013.00179.

Bridges, R.J., Natale, N.R., Patel, S.A., 2012. System xc- cystine/glutamate antiporter: an update on molecular pharmacology and roles within the CNS: system xc- cystine/glutamate antiporter. Br. J. Pharmacol. 165, 20–34. https://doi.org/10.1111/j.1476-5381.2011.01480.x.

Browne, R.W., Armstrong, D., 1998. Reduced glutathione and glutathione disulfide. Methods Mol. Biol. 108, 347–352. https://doi.org/10.1385/0-89603-472-0:347.

Brozzi, F., Arcuri, C., Giambanco, I., Donato, R., 2009. S100B protein regulates astrocyte shape and migration via interaction with Src Kinase: IMPLICATIONS for astrocyte development, activation, and tumor growth. J. Biol. Chem. 284, 8797–8811. https://doi.org/10.1074/jbc.M805897200.

Budunova, I.V., Williams, G.M., 1994. Cell culture assays for chemicals with tumor-promoting or tumor-inhibiting activity based on the modulation of intercellular communication. Cell Biol. Toxicol. 10, 71–116. https://doi.org/10.1007/BF00756491.

De Pittà, M., Brunel, N., Volterra, A., 2016. Astrocytes: orchestrating synaptic plasticity? Neuroscience 323, 43–61. https://doi.org/10.1016/j.neuroscience.2015.04.001.

Dringen, R., Brandmann, M., Hohnholt, M.C., Blumrich, E.-M., 2015. Glutathione-dependent detoxification processes in astrocytes. Neurochem. Res. 40, 2570–2582. https://doi.org/10.1007/s11064-014-1481-1.

Eng, L.F., 1985. Glial fibrillary acidic protein (GFAP): the major protein of glial intermediate filaments in differentiated astrocytes. J. Neuroimmunol. 8, 203–214. https://doi.org/10.1016/S0165-5728(85)80063-1.

Frisa, P.S., Jacobberger, J.W., 2002. Cell density related gene expression: SV40 large T antigen levels in immortalized astrocyte lines. BMC Cell Biol. 3, 10. https://doi.org/10.1186/1471-2121-3-10.

Furihata, T., Ito, R., Kamiichi, A., Saito, K., Chiba, K., 2016. Establishment and characterization of a new conditionally immortalized human astrocyte cell line. J. Neurochem. 136, 92–105. https://doi.org/10.1111/jnc.13358.

Geller, H.M., Dubois-Dalcq, M., 1988. Antigenic and functional characterization of a rat central nervous system-derived cell line immortalized by a retroviral vector. J. Cell Biol. 107, 1977–1986. https://doi.org/10.1083/jcb.107.5.1977.

Gottfried, C., Tramontina, F., Gonçalves, D., Gonçalves, C.A., Moriguchi, E., Dias, R.D., Wofchuk, S.T., Souza, D.O., 2002. Glutamate uptake in cultured astrocytes depends on age: a study about the effect of guanosine and the sensitivity to oxidative stress induced by H(2)O(2). Mech. Ageing Dev. 123, 1333–1340. https://doi.org/10.1016/S0047-6374(02)00069-6.

Groves, A.K., Entwistle, A., Jat, P.S., Noble, M., 1993. The characterization of astrocyte cell lines that display properties of glial scar tissue. Dev. Biol. 159, 87–104. https://doi.org/10.1006/dbio.1993.1223.

Haghighat, N., 2005. Estrogen (17beta-estradiol) enhances glutamine synthetase activity in C6-glioma cells. Neurochem. Res. 30, 661–667. https://doi.org/10.1007/s11064-005-2754-5.

Haghighat, N., McCandless, D.W., 1997a. Effect of 6-aminonicotinamide on metabolism of astrocytes and C6-glioma cells. Metab. Brain Dis. 12, 29–45. https://doi.org/10.1007/BF02676352.

Haghighat, N., McCandless, D.W., 1997b. Effect of ammonium chloride on energy metabolism of astrocytes and C6-glioma cells in vitro. Metab. Brain Dis. 12, 287–298. https://doi.org/10.1007/BF02674673.

Hertz, L., Chen, Y., Song, D., 2017. Astrocyte cultures mimicking brain astrocytes in gene expression, signaling, metabolism and K(+) uptake and showing astrocytic gene expression overlooked by immunohistochemistry and in Situ hybridization. Neurochem. Res. 42, 254–271. https://doi.org/10.1007/s11064-016-1828-x.

Johnson, K.M., Milner, R., Crocker, S.J., 2015. Extracellular matrix composition determines astrocyte responses to mechanical and inflammatory stimuli. Neurosci. Lett. 600, 104–109. https://doi.org/10.1016/j.neulet.2015.06.013.

Krupenko, S.A., 2009. FDH: an aldehyde dehydrogenase fusion enzyme in folate metabolism. Chem. Biol. Interact. 178, 84–93. https://doi.org/10.1016/j.cbi.2008.09.007.

Labak, C.M., Wang, P.Y., Arora, R., Guda, M.R., Asuthkar, S., Tsung, A.J., Velpula, K.K., 2016. Glucose transport: meeting the metabolic demands of cancer, and applications in glioblastoma treatment. Am. J. Cancer Res.

Lange, S.C., Bak, L.K., Waagepetersen, H.S., Schousboe, A., Norenberg, M.D., 2012. Primary cultures of astrocytes: their value in understanding astrocytes in health and disease. Neurochem. Res. 37, 2569–2588. https://doi.org/10.1007/s11064-012-0868-0.

Lasič, E., Galland, F., Vardjan, N., Šribar, J., Križaj, I., Leite, M.C., Zorec, R., Stenovec, M., 2016. Time-dependent uptake and trafficking of vesicles capturing extracellular S100B in cultured rat astrocytes. J. Neurochem. https://doi.org/10.1111/jnc.13754.

Leite, M.C., Galland, F., Brolese, G., Guerra, M.C., Bortolotto, J.W., Freitas, R., Almeida, L.M.V.d., Gottfried, C., Gonçalves, C.-A., 2008. A simple, sensitive and widely applicable ELISA for S100B: methodological features of the measurement of this glial protein. J. Neurosci. Methods 169. https://doi.org/10.1016/j.jneumeth.2007.11.021.

Leite, M.C., Galland, F., De Souza, D.F., Guerra, M.C., Bobermin, L., Biasibetti, R.,

Gottfried, C., Gonçalves, C.-A., 2009. Gap junction inhibitors modulate S100B secretion in astrocyte cultures and acute hippocampal slices. J. Neurosci. Res. 87. https://doi.org/10.1002/jnr.22083.
Liu, L., Gao, Z., Zhang, L., Su, L., Dong, G., Yu, H., Tian, J., Zhao, H., Xu, Y., Liu, H., 2012. Temporal dynamic changes of connexin 43 expression in C6 cells following lipopolysaccharide stimulation. Neural Regen Res 7, 1947–1953. https://doi.org/10.3969/j.issn.1673-5374.2012.25.004.
Marie, S.K., Shinjo, S.M., 2011. Metabolism and brain cancer. Clin. (Sao Paulo) 66 (Suppl. 1), 33–43. https://doi.org/10.1590/S1807-59322011001300005.
Matés, J.M., Pérez-Gómez, C., Núñez de Castro, I., Asenjo, M., Márquez, J., 2002. Glutamine and its relationship with intracellular redox status, oxidative stress and cell proliferation/death. Int. J. Biochem. Cell Biol. 34, 439–458. https://doi.org/10.1016/S1357-2725(01)00143-1.
McKenna, M.C., Sonnewald, U., Huang, X., Stevenson, J., Zielke, H.R., 1996. Exogenous glutamate concentration regulates the metabolic fate of glutamate in astrocytes. J. Neurochem. 66, 386–393. https://doi.org/10.1046/j.1471-4159.1996.66010386.x.
Menet, V., Giménez y Ribotta, M., Chauvet, N., Drian, M.J., Lannoy, J., Colucci-Guyon, E., Privat, A., 2001. Inactivation of the glial fibrillary acidic protein gene, but not that of vimentin, improves neuronal survival and neurite growth by modifying adhesion molecule expression. J. Neurosci. 21, 6147–6158. https://doi.org/10.1523/JNEUROSCI.21-16-06147.2001.
Minet, R., Villie, F., Marcollet, M., Meynial-Denis, D., Cynober, L., 1997. Measurement of glutamine synthetase activity in rat muscle by a colorimetric assay. Clin. Chim. Acta 268, 121–132. https://doi.org/10.1016/s0009-8981(97)00173-3.
Morikawa, M., Asai, K., Kokubo, M., Fujita, K., Yoneda, K., Yamamoto, N., Inoue, Y., Iida, J., Kishimoto, T., Kato, T., 2001. Isolation and characterization of a new immortal rat astrocyte with a high expression of NGF mRNA. Neurosci. Res. 39, 205–212. https://doi.org/10.1016/S0168-0102(00)00217-0.
Nardin, P., Tramontina, F., Leite, M.C., Tramontina, A.C., Quincozes-Santos, A., de Almeida, L.M., Battastini, A.M., Gottfried, C., Gonçalves, C.A., 2007. S100B content and secretion decrease in astrocytes cultured in high-glucose medium. Neurochem. Int. 50, 774–782. https://doi.org/10.1016/j.neuint.2007.01.013.
Olsen, M.L., Sontheimer, H., 2008. Functional implications for Kir4.1 channels in glial biology: from K+ buffering to cell differentiation. J. Neurochem. 107, 589–601. https://doi.org/10.1111/j.1471-4159.2008.05615.x.
Ostroff, L.E., Manzur, M.K., Cain, C.K., Ledoux, J.E., 2014. Synapses lacking astrocyte appear in the amygdala during consolidation of Pavlovian threat conditioning. J. Comp. Neurol. 522, 2152–2163. https://doi.org/10.1002/cne.23523.
Pallardó, F.V., Markovic, J., García, J.L., Viña, J., 2009. Role of nuclear glutathione as a key regulator of cell proliferation. Mol. Asp. Med. 30, 77–85. https://doi.org/10.1016/j.mam.2009.01.001.
Palos, T.P., Ramachandran, B., Boado, R., Howard, B.D., 1996. Rat C6 and human astrocytic tumor cells express a neuronal type of glutamate transporter. Brain Res Mol Brain Res 37, 297–303. https://doi.org/10.1016/0169-328X(95)00331-L.
Papadopoulos, M.C., Verkman, A.S., 2013. Aquaporin water channels in the nervous system. Nat. Rev. Neurosci. 14, 265–277. https://doi.org/10.1038/nrn3468.
Parker, K.K., Norenberg, M.D., Vernadakis, A., 1980. Transdifferentiation" of C6 glial cells in culture. Science 208, 179–181. https://doi.org/10.1126/science.6102413.
Passaquin, A.C., Schreier, W.A., de Vellis, J., 1994. Gene expression in astrocytes is affected by subculture. Int. J. Dev. Neurosci. 12, 363–372. https://doi.org/10.1016/0736-5748(94)90086-8.
Pellerin, L., 2008. Brain energetics (thought needs food). Curr. Opin. Clin. Nutr. Metab. Care 11, 701–705. https://doi.org/10.1097/MCO.0b013e328312c368.
Pellerin, L., Magistretti, P.J., 1994. Glutamate uptake into astrocytes stimulates aerobic glycolysis: a mechanism coupling neuronal activity to glucose utilization. Proc. Natl. Acad. Sci. U. S. A. 91, 10625–10629. https://doi.org/10.1073/pnas.91.22.10625.
Peterson, G.L., 1977. A simplification of the protein assay method of Lowry et al. which is more generally applicable. Anal. Biochem. 83, 346–356. https://doi.org/10.1016/0003-2697(77)90043-4.
Pinto, S.S., Gottfried, C., Mendez, A., Gonçalves, D., Karl, J., Gonçalves, C.A., Wofchuk, S., Rodnight, R., 2000. Immunocontent and secretion of S100B in astrocyte cultures from different brain regions in relation to morphology. FEBS Lett. 486, 203–207. https://doi.org/10.1016/s0014-5793(00)02301-2.
Raju, T.R., Bignami, A., Dahl, D., 1980. Glial fibrillary acidic protein in monolayer cultures of C-6 glioma cells: effect of aging and dibutyryl cyclic AMP. Brain Res. 200, 225–230. https://doi.org/10.1016/0006-8993(80)91114-2.
Rouach, N., Avignone, E., Même, W., Koulakoff, A., Venance, L., Blomstrand, F., Giaume, C., 2002. Gap junctions and connexin expression in the normal and pathological central nervous system. Biol. Cell 94, 457–475. https://doi.org/10.1016/S0248-4900(02)00016-3.
Sánchez-Alvarez, R., Tabernero, A., Medina, J.M., 2004. Endothelin-1 stimulates the translocation and upregulation of both glucose transporter and hexokinase in astrocytes: relationship with gap junctional communication. J. Neurochem. https://doi.org/10.1046/j.1471-4159.2004.02398.x.
Seifert, G., Henneberger, C., Steinhäuser, C., 2016. Diversity of astrocyte potassium channels: an update. Brain Res. Bull. https://doi.org/10.1016/j.brainresbull.2016.12.002.
Souza, D.G., Bellaver, B., Souza, D.O., Quincozes-Santos, A., 2013. Characterization of adult rat astrocyte cultures. PLoS One 8, e60282. https://doi.org/10.1371/journal.pone.0060282.
Tabernero, A., Medina, J.M., Giaume, C., 2006. Glucose metabolism and proliferation in glia: role of astrocytic gap junctions. J. Neurochem. 99, 1049–1061. https://doi.org/10.1111/j.1471-4159.2006.04088.x.
Tabuchi, K., Imada, M., Nishimoto, A., 1982. Effects of cyclic AMP on S-100 protein level in C-6 glioma cells. J. Neurol. Sci. 56, 57–63. https://doi.org/10.1016/0022-510X(82)90060-0.
Thomazi, A.P., Godinho, G.F., Rodrigues, J.M., Schwalm, F.D., Frizzo, M.E., Moriguchi, E., Souza, D.O., Wofchuk, S.T., 2004. Ontogenetic profile of glutamate uptake in brain structures slices from rats: sensitivity to guanosine. Mech. Ageing Dev. 125, 475–481. https://doi.org/10.1016/j.mad.2004.04.005.
Trabelsi, Y., Amri, M., Becq, H., Molinari, F., Aniksztejn, L., 2017. The conversion of glutamate by glutamine synthase in neocortical astrocytes from juvenile rat is important to limit glutamate spillover and peri/extrasynaptic activation of NMDA receptors. Glia 65, 401–415. https://doi.org/10.1002/glia.23099.
Tramontina, F., Leite, M.C., Cereser, K., de Souza, D.F., Tramontina, A.C., Nardin, P., Andreazza, A.C., Gottfried, C., Kapczinski, F., Gonçalves, C.-A., Goncalves, C.A., 2007. Immunoassay for glial fibrillary acidic protein: antigen recognition is affected by its phosphorylation state. J. Neurosci. Methods 162, 282–286. https://doi.org/10.1016/j.jneumeth.2007.01.001.
Turnquist, C., Horikawa, I., Foran, E., Major, E.O., Vojtesek, B., Lane, D.P., Lu, X., Harris, B.T., Harris, C.C., 2016. p53 isoforms regulate astrocyte-mediated neuroprotection and neurodegeneration. Cell Death Differ. 23, 1515–1528. https://doi.org/10.1038/cdd.2016.37.
Van Eldik, L.J., Wainwright, M.S., 2003. The Janus face of glial-derived S100B: beneficial and detrimental functions in the brain. Restor. Neurol. Neurosci. 21, 97–108.
Vanhoutte, N., Hermans, E., 2008. Glutamate-induced glioma cell proliferation is prevented by functional expression of the glutamate transporter GLT-1. FEBS Lett. 582, 1847–1852. https://doi.org/10.1016/j.febslet.2008.04.053.
Wilhelmsson, U., Li, L., Pekna, M., Berthold, C.H., Blom, S., Eliasson, C., Renner, O., Bushong, E., Ellisman, M., Morgan, T.E., Pekny, M., 2004. Absence of glial fibrillary acidic protein and vimentin prevents hypertrophy of astrocytic processes and improves post-traumatic regeneration. J. Neurosci. 24, 5016–5021. https://doi.org/10.1523/JNEUROSCI.0820-04.2004.
Yang, Y., Vidensky, S., Jin, L., Jie, C., Lorenzini, I., Frankl, M., Rothstein, J.D., 2011. Molecular comparison of GLT1+ and ALDH1L1+ astrocytes in vivo in astroglial reporter mice. Glia 59, 200–207. https://doi.org/10.1002/glia.21089.
Zhou, D., Jiang, X., Xu, R., Cai, Y., Hu, J., Xu, G., Zou, Y., Zeng, Y., 2008. Assessing the cytoskeletal system and its elements in C6 glioma cells and astrocytes by atomic force microscopy. Cell. Mol. Neurobiol. 28, 895–905. https://doi.org/10.1007/s10571-008-9267-0.